



Removal of residual contaminants in petroleum-contaminated soil by Fenton-like oxidation

Mang Lu^{a,b}, Zhongzhi Zhang^{b,*}, Wei Qiao^b, Yueming Guan^b, Meng Xiao^b, Chong Peng^b

^a School of Material Science and Engineering, Jingdezhen Ceramic Institute, Jingdezhen, 333001, Jiangxi Province, China

^b State Key Laboratory of Heavy Oil Processing, China University of Petroleum, Beijing 102249, China

ARTICLE INFO

Article history:

Received 19 December 2009

Received in revised form 10 March 2010

Accepted 10 March 2010

Available online 17 March 2010

Keywords:

Bioremediation residues

EDTA

Infrared spectra

Fourier transform ion cyclotron resonance mass spectrometry

ABSTRACT

The degradation of bioremediation residues by hydrogen peroxide in petroleum-contaminated soil was investigated at circumneutral pH using a Fenton-like reagent (ferric ion chelated with EDTA). Batch tests were done on 20 g soil suspended in 60 mL aqueous solution containing hydrogen peroxide and Fe³⁺–EDTA complex under constant stirring. A slurry reactor was used to treat the soil based on the optimal reactant conditions. Contaminants were characterized by Fourier transform infrared spectroscopy and Fourier transform ion cyclotron resonance mass spectrometry. The results showed that the optimal treatment condition was: the molar ratio of hydrogen peroxide to iron = 200:1, and pH 7.0. Under the optimum condition, total dichloromethane-extractable organics were reduced from 14,800 to 2300 mg kg⁻¹ soil when the accumulative H₂O₂ dosage was 2.45 mol kg⁻¹ soil during the reactor treatment. Abundance of viable cells was lower in incubated Fenton-like treated soil than in untreated soil. Oxidation of contaminants produced remarkable compositional and structural modifications. A fused ring compound, identified as C₃₄H₃₈N₁, was found to exhibit the greatest resistance to oxidation.

© 2010 Elsevier B.V. All rights reserved.

1. Introduction

Bioremediation may remove the contaminants to a large extent and has proven successful in many applications to petroleum-contaminated soils. However, bioremediation is often unable to reduce the level of contamination and long-term soil toxicity below the stringent cleanup standards dictated by environmental regulations [1]. Moreover, petroleum cannot be completely mineralized to CO₂ and H₂O by soil microorganisms, and always leaves more or less complex residues [2].

The rate and extent of petroleum biodegradation is dependent on a variety of factors, including the physical conditions and the nature, concentration, and ratios of various structural classes of hydrocarbons present, the bioavailability of the substrate, inhibitory substrates or metabolites, and the metabolic potential of microorganisms to detoxify or utilize the contaminant involved [3,4]. Changes of chemical concentration resulting from bioremediation usually follow the pattern of an initial period of rapid degradation followed by a zero or very slow rate of change. Loss of contaminants occurs slowly once this apparent concentration plateau has been reached [5]. In addition, undetected metabolites or compounds may be formed during the biodegradation process [1]. These metabolites consist of fatty acids, naphthenic acids, and

oxygenated polycyclic aromatic hydrocarbons, etc., and degradation may be inhibited in the presence of these compounds due to the suppressed microbial degradative activity [6–8].

An efficient approach to the removal of bioremediation residues may be the application of a strong oxidizing agent such as Fenton's reagent (Fe²⁺ + H₂O₂). Fenton oxidation may not only destroy target compounds, but also reduce toxicity [9]. This chemical oxidation approach is recognized as one of the most powerful oxidizing reactions available and can be used to destroy a wide variety of biorefractory organic compounds in aqueous waste, soils, and ground water. However, one limitation of the original Fenton's process is that the optimal pH range to maximize oxidation of target compounds is approximately 3.0–4.0, which necessitates pH adjustments before and after treatment. Organic chelating agents such as catechol, gallic acid, cyclodextrins, and ethylenediaminetetraacetic acid (EDTA) can be added to modified Fenton systems to maintain adequate degradation rates in the pH range of 6.0–9.0 [10–12].

Recently, there are many studies published on the Fenton-like remediation of petroleum-contaminated soils [13–16]. These studies were mainly focused on selecting the optimal catalyst systems, and/or optimizing process parameters such as the dosage of oxidant and catalyst and their ratios. However, there is a lack of information about changes in the chemical composition of petroleum and derivatives, especially hetero atomic compounds. In this paper, we applied a Fenton-like process to destroy residual contaminants in petroleum-contaminated soil after bioremediation. The optimum

* Corresponding author. Tel.: +86 10 89734284; fax: +86 10 69744636.
E-mail address: zzzhang1955@hotmail.com (Z. Zhang).

Table 1
Characteristics of the contaminated soil after composting.

Characteristic	Concentration
Sand (%)	17.3
Clay (%)	22.5
Silt (%)	60.2
Crystalline Mn oxides (mg kg ⁻¹)	2460
Crystalline Fe oxides (mg kg ⁻¹)	15,700
Amorphous Mn oxides (mg kg ⁻¹)	78.3
TEO	14,800

ratio between H₂O₂ and catalyst was determined with batch experiments. In addition, we used a powerful and relatively new approach—electrospray ionization Fourier transform ion cyclotron resonance mass spectrometry (ESI FT-ICR MS) to monitor compositional changes of the contaminants during the Fenton-like treatment. By this approach the molecular formulas of compounds contained in complex mixtures can be estimated by FT-ICR MS without chromatographic fractionation of the sample. Moreover, ESI allows polar compounds to be distinguished without the need for derivatization, eliminating the need to correct for isotope distributions in the derivatizing agent.

2. Materials and methods

2.1. Soil

The contaminated soil was initially collected from the adjacent areas of oil wells in Dagang Oilfield (Tianjing, China, latitude 38°34'N and longitude 116°43'E), which had a silt loam texture, pH of 7.7 (1:2 ratio of dry soil to distilled water). Contaminated soil was removed from 15 to 45 cm depth layer and sieved through a 2-mm screen. Soil was stored at 4 °C in the dark until required.

The soil had been biotreated using composting for two years previously (unpublished results). The initial concentration of total dichloromethane-extractable organics (TEO) in the soil before composting was 32,300 mg kg⁻¹. However, the contamination level was still high, and the reduction of contamination had reached a plateau for a long time.

The previous composting process was as follows: the soil was stacked with sawdust in separate piles of approximately 30–35 cm height and 1.5 m width; NPK fertilizer (20:20:20), composed of urea phosphate, potassium nitrate and ammonium nitrate, was applied to fertilize all the treatments; the ambient temperature during the preparation work was 15–30 °C; a mixed culture of microorganisms isolated from crude oil-contaminated soil was used as inoculum. This culture has been used in the treatment of oilfield produced water with high salinity in pilot scale in a previous study [17]. Characteristics of the soil after composting were shown in Table 1.

Gas chromatography/mass spectrometry analysis suggested that there existed large area of the unresolved complex mixture “hump” under the resolved peak envelope, which might be indicative of the presence of a large amount of metabolites (further details are shown in Supporting information, Section 1).

2.2. Optimization of Fenton-like process

The degradation of bioremediation residues in soil by Fenton-like treatment was optimized under batch conditions. EDTA is the mostly used chelating agent in the Fenton-chelate based studies at neutral pH because of its high efficiency in the enhancement of the degradation of hydrophobic organic contaminants under Fenton's chemistry [18]. In this study, therefore, the Fe³⁺–EDTA complex was used as a catalyst to provide the Fenton-like reaction. The Fe³⁺–EDTA complex was made daily using a 1:1 molar ratio of EDTA to iron. The EDTA was dissolved in deionized water and sodium

hydroxide at a 4:1 molar ratio. After dissolution of EDTA, the pH was adjusted to 3 using dilute sulfuric acid and the Fe₂(SO₄)₃ was added to the solution.

It is well documented that sequential addition of hydrogen peroxide is more effective and economical than addition of hydrogen peroxide all at once in soil remediation [10,13]. Hence a relatively small fixed dose of hydrogen peroxide was applied while changing pH and the dose of iron to obtained optimum reaction conditions. Briefly, a mass of 20 g of soil was weighed into a 250-mL Erlenmeyer flask and then 59 mL of deionized water was added. The flasks were shaken at 150 rpm for 2 h to ensure homogenization. After this period, the desired amount of the catalyst was added to the slurry in a concentrated aqueous form (0.1 mL). Slurry pH was adjusted to 6.0, 7.0, and 7.5 respectively with dilute sulfuric acid. Subsequently, each flask received 1 mL of 30% H₂O₂ (w/v), namely the hydrogen peroxide dose was fixed at 0.49 mol kg⁻¹ soil. The molar ratio of H₂O₂:Fe³⁺ ranged from 50:1 to 400:1. The flasks were placed on a reciprocating shaker at 150 rpm for 24 h at 25 °C under dark conditions.

2.3. Fenton-like treatment in a slurry reactor

The subsequent experiment was performed in a slurry reactor based on the optimum process conditions found above. The reactor consisted of a 7-L round-bottom Pyrex glass vessel with an adjustable fitted cover. The reactor received 1.5 kg of soil and 4425 mL of distilled water. The pH was adjusted to 7.0 with sulfuric acid and the reactor was maintained with stirring at 600 rpm. The soil slurry, before addition of chemical reagent, was equilibrated for 2 h in the reactor. The reagent was added in a single batch at 24-h interval. Each time, the reactor received 75 mL of 30% H₂O₂ (0.49 mol kg⁻¹ soil) and the corresponding optimal dose of concentrated Fe³⁺–EDTA solution. This addition did not significantly change the volume of slurry over the time of soil treatment. The temperature was maintained at 25 °C in the dark. The pH in the slurry reactor was controlled at the designated pH (7 ± 0.1) during the course of reaction using a pH controller (DT-1023, Biott) and addition of 1 M H₂SO₄ or NaOH.

2.4. Sampling and analysis

The soil and aqueous phase were not separated before extraction. The total mass of contaminants in the entire mixture was extracted by the conventional Soxhlet extraction as follows: soil or slurry was oven dried at 45 °C for 24 h and then further dried with anhydrous sodium sulfate and extracted with chromatographic-grade dichloromethane for 8 h using a Soxhlet apparatus. Solvent was evaporated at 30 °C under a nitrogen stream. TEO was determined gravimetrically after solvent evaporation [19].

After extraction, an aliquot of TEO was examined by FT-IR and ESI FT-ICR MS. For FT-IR analysis, TEO samples were dissolved in chloroform and cast on KBr plates. FT-IR spectra were recorded on a Nicolet Avatar 360 Fourier transform infrared (USA) spectroscope. The FT-IR spectrum was collected between the wave number of 400 and 4000 cm⁻¹.

FT-ICR MS analysis was performed on an Apex-ultra FT-ICR MS (Bruker Daltonics, USA) equipped with a 9.4T actively shielded magnet. The TEO sample was dissolved in dichloromethane at a concentration of 0.1 mg mL⁻¹. A 1-mL aliquot of this solution was diluted with 1 mL of methanol, and then spiked with 10 μL of 35% (v/v) conc. NH₄OH to facilitate deprotonation of acidic compounds by negative ion electrospray. The analysis was performed on an Apex-ultra FT-ICR MS (Bruker Daltonics, USA) equipped with a 9.4T actively shielded magnet. Ions were generated by negative ion electrospray equipped with a 50 μm i.d. fused silica ESI needle. Samples were infused at a flow rate of 250 μL h⁻¹. The operating software

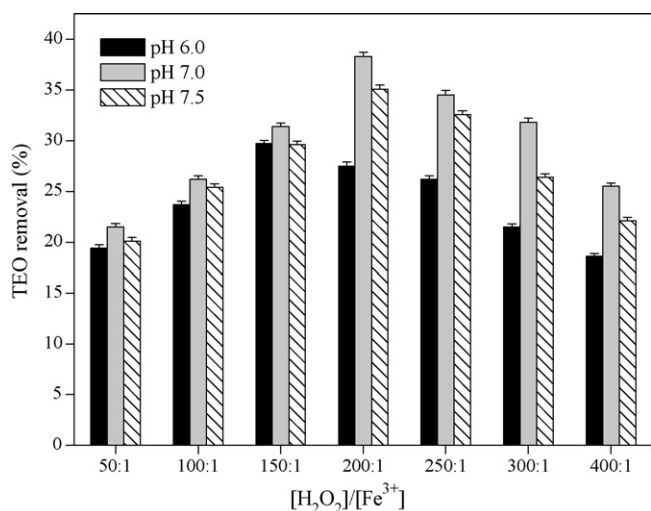


Fig. 1. Effect of $[H_2O_2]:[Fe^{3+}]$ and pH on TEO mass removal. Reported values are the mean \pm one standard deviation ($n=3$). The hydrogen peroxide dose was fixed at 0.49 mol kg^{-1} soil.

was XMASS version 6.0 (Bruker Daltonics, USA). Each spectrum was composed of 64 scans. Data collection and compound searching were performed using the software programmed by Analysis Center, State Key Laboratory of Heavy Oil Processing, China University of Petroleum.

The FT-ICR mass spectra were acquired using standard experimental sequences as provided by the manufacturer. FT-ICR MS data analysis was conducted according to Hughey et al. [20]. Once a homologous series is identified, it is described by its class (heteroatom content) and the number of rings plus double bonds. The number of rings plus double bonds is commonly described by a Z value. The Z value decreases by two units for each additional ring plus double bond. For a compound with the molecular formula C_cH_nX (where X refer to the heteroatom present such as N and O) the Z value is determined by

$$Z = h - 2c \quad (1)$$

2.5. Microbial enumeration

Before and after the slurry reactor treatment, total heterotrophic bacteria in the soil were quantified using the drop plate method of Cassidy et al. [21] with $20 \mu\text{L}$ per drop over a range of serial dilutions on nutrient agar supplemented with 75 mg L^{-1} cycloheximide to inhibit fungal growth. Plates were incubated at 30°C for 24 h in the dark and colonies counted. Microbial counts were expressed as colony-forming units (CFU) g^{-1} soil.

2.6. Data analysis

All experiments were carried out in triplicate to get reliable data and the results presented here represent average of three independent measurements. All results of soil were expressed on an oven-dry (105°C , 24 h), dichloromethane-extracted soil mass basis.

3. Results and discussion

3.1. Effect of iron levels and pH on contaminant removal

The removal of soil TEO in batch tests is presented in Fig. 1. It may be observed that an increasing percentage of oxidation was obtained with decreasing concentration of Fe^{3+} at the three pHs studied. An excess of Fe^{3+} in the solution may cause unproductive

consumption of hydroxyl radicals. Moreover, EDTA can also consume a certain number of hydroxyl radicals, since hydroxyl radicals non-specifically oxidize the organic compounds [22]. However, it may be observed that once the ratio of $H_2O_2:Fe^{3+}$ had reached 150 (pH 6.0) or 200 (pH 7.0 and 7.5), the removal levels of TEO decreased as the concentration of iron diminished. This result was attributed to the reduced availability of soluble iron as a result of precipitation after oxidation of the chelating agent. Moreover, another reason for TEO removal reduction could be the excess of hydrogen peroxide providing the conditions for increased quenching of hydroxyl radicals. After addition of H_2O_2 , pH values of flask contents slightly decreased by 0.1 units, which came back to the initial values at the end of the test.

Under different initial pH conditions, the best results of the residues degradation were obtained at pH 7.0, with the maximum removal of 38.3% at the molar ratio of $H_2O_2:Fe^{3+} = 200:1$. This optimum molar ratio of $H_2O_2:Fe^{3+}$ was 150:1 at pH 6.0 and 7.5, respectively. The catalyst seemed to be less active at pH 6.0 than at pH 7.0. Lou and Huang [22] demonstrated that the destruction efficacy of EDTA increased with decreasing pH due to the enhanced generation of hydroxyl radicals. In the present study, the degradation of EDTA might be quicker at pH 6.0 than at pH 7.0, which caused the precipitation of ferric iron. Curiously, the removal efficacy of TEO was lower at pH 7.5 than at pH 7.0, indicating that Fe^{3+} -EDTA might be less active at high pH.

Based on the above batch experiment, the optimum reaction conditions were estimated: a pH of 7.0, and a molar ratio of $H_2O_2:Fe^{3+} = 200:1$.

3.2. Effect of H_2O_2 dosage on TEO removal in slurry reactor treatment

The bench-scale experiment was conducted in the slurry reactor based on the optimum process conditions found above: pH 7.0, and $H_2O_2:Fe^{3+}$ molar ratio of 200:1. It was found that the removal of TEO in the soil increased with increasing dosage of H_2O_2 (Fig. 2). TEO decreased to 4060 mg kg^{-1} soil when H_2O_2 dosage was 1.47 mol kg^{-1} soil. While H_2O_2 dosage was further elevated, TEO removal did not increase much significantly. Finally, TEO was reduced to 2300 mg kg^{-1} soil when H_2O_2 dosage was 2.45 mol kg^{-1} soil. The value is below the national environmental standard for agricultural soil: $<3000 \text{ mg kg}^{-1}$ for petroleum and derivatives (Environmental Quality Standard for Soils of China, GB15618–1995). Therefore, it is safe for crop production accord-

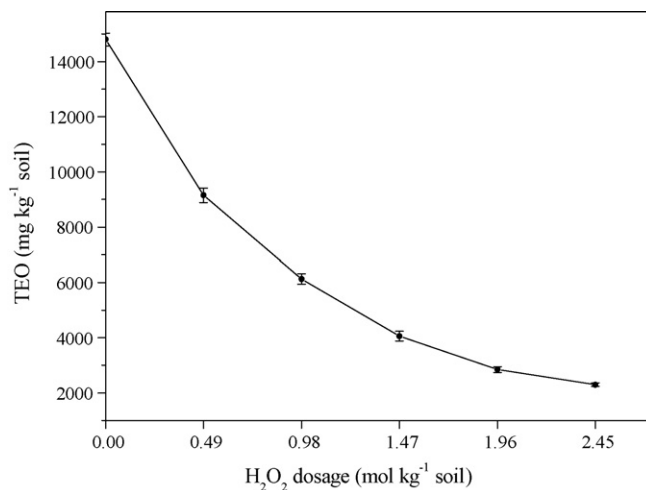


Fig. 2. Cumulative quantity of TEO removal during Fenton-like oxidation treatment in the slurry reactor at pH 7. Each dose was 0.49 mol kg^{-1} soil.

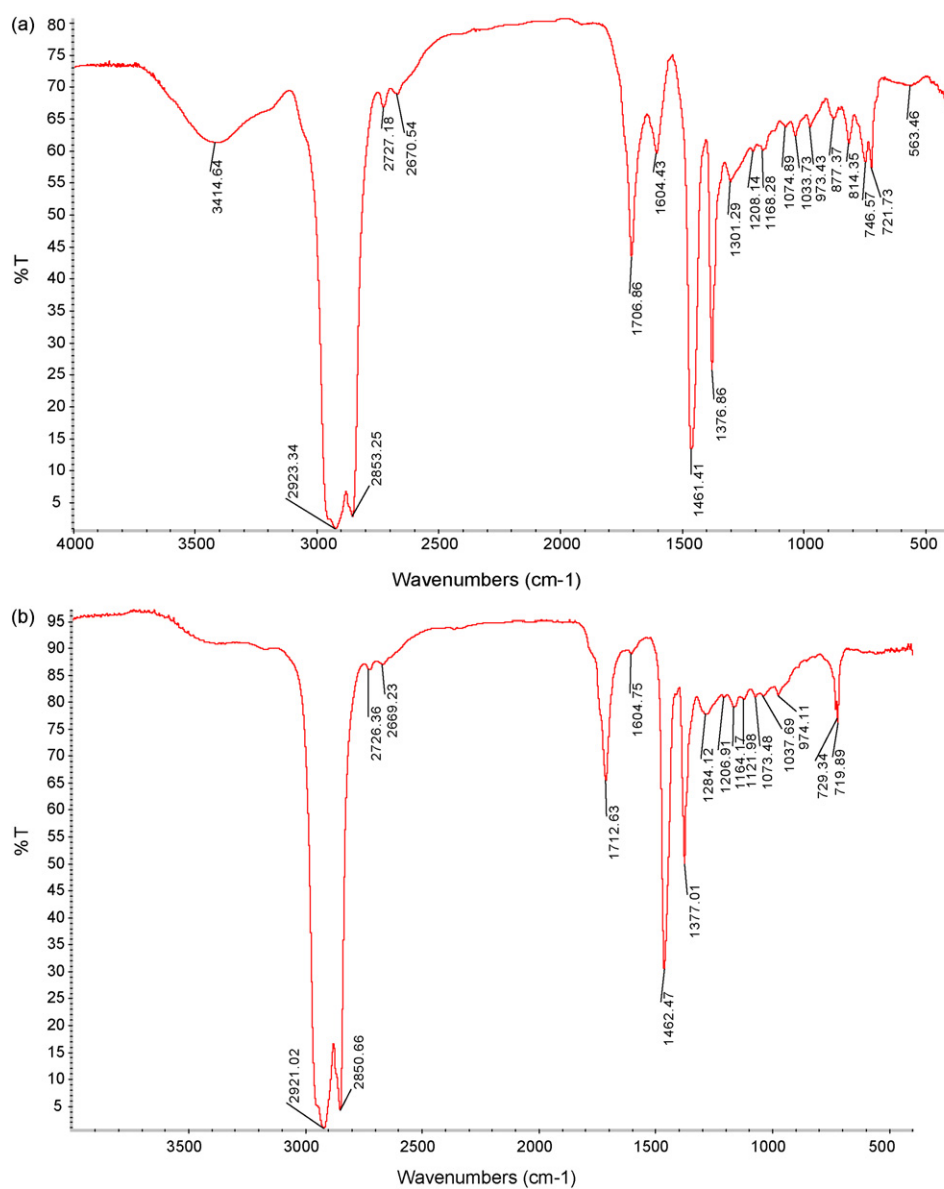


Fig. 3. FT-IR spectra of TEO. (a) Before oxidation, and (b) after oxidation.

ing to present regulations. In fact, higher removal efficacy could be achieved with a larger quantity of reagent. However the residues became more and more difficult to be oxidized with the proceeding of oxidation.

3.3. Effect of Fenton-like oxidation on survival of bacteria

The soil had a baseline population of 5.28×10^6 CFU g⁻¹ soil, which dropped to 4.50×10^3 CFU g⁻¹ soil as a result of Fenton-like oxidation (data not shown). Treatment of soil with the Fenton-like reaction resulted in significant loss of the number of soil microorganisms detected. Hydrogen peroxide is toxic to microorganisms and is usually used as an effective disinfectant in medical practice. However, many microorganisms have superoxide dismutase enzymes that scavenge excess superoxide and catalase enzymes that decompose hydrogen peroxide, preventing the formation of hydroxyl radicals and/or intracellular transport of free iron [23]. In this study, therefore, there still existed a certain amount of viable cells which had survived from strong oxidation reactions.

3.4. Infrared spectrometry

Fig. 3 shows FT-IR spectra before and after Fenton-like oxidation. The infrared spectrum of TEO (before oxidation) showed the characteristic bands of aliphatic (CH₂ and CH₃ stretching at 2923 and 2863 cm⁻¹, CH₂ and CH₃ bending at 1462 and 1377 cm⁻¹), aromatic rings (ring stretching at 1604 cm⁻¹, CH out-of-plane bending at 563, 720, and 746 cm⁻¹), and carboxylic acids (carbonyl stretching at 1707 cm⁻¹, COOH complex pattern between 3500 and 2400 cm⁻¹) [24]. A broad band centred on 3400 cm⁻¹ is due to the hydrogen vibrations of alcoholic OH, phenol or carboxyl groups (COOH), but also to N–H vibrations of amides. The band centred on 1033 cm⁻¹ is attributed to aromatic ethers. The C–N stretching vibrations of the primary amino groups are detected at about 1301 and 1074 cm⁻¹. The band at 1208 cm⁻¹ is assigned to amide coupled with hydrocarbon skeleton. The band at 877 cm⁻¹ suggests the presence of penta-substituted aromatic rings containing isolated CH bonds. The band at 814 cm⁻¹ is attributed to the contribution of the aromatic rings that contain two and three adjacent aromatic CH groups.

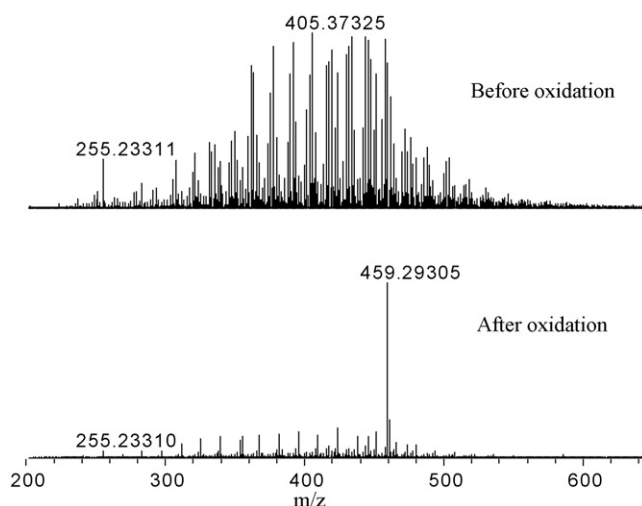


Fig. 4. Broadband negative ion ESI FT-ICR mass spectra of the bioremediation residues. Peaks identified have a threshold greater than 3σ the baseline noise.

In our experiment, the intensity of some bands was changed with the oxidation progress. The IR bands of OH groups (3414 cm^{-1}) decreased obviously. The intensities of bands at 1377 cm^{-1} and between 2921 and 2669 cm^{-1} did not change significantly. However, the aromatic bands intensity in the 1604 cm^{-1} region decreased drastically as could correspond to oxidation or transformation of aromatic structures. There was an overall decrease in the alkyl chain length with chemical oxidation (ratio of 1370 – 1390 to 1430 – 1470 cm^{-1}).

3.5. FT-ICR mass spectra

The calibrated negative-ion FT-ICR mass spectra of TEO samples are presented in Fig. 4. In each spectrum, more than 13,000 peaks with a signal to noise ratio of greater than 3 were detected in the range. The mass spectra clearly showed that the contamination level was greatly reduced by Fenton-like oxidation. Interestingly, the ion at m/z 459.29305 became the most abundant after oxidation, which amazingly accounted for 5.49% of the total ion intensity. This peak was identified as $\text{C}_{34}\text{H}_{38}\text{N}_1$ (error 0.1 ppm), which has a Z value of -30 , indicating the presence of fused rings in its molecular structure.

From the mass spectra, a wide variety of compounds were identified (Table 3). O_2 -species were the predominant species both before and after treatment. The Fenton-like treatment altered compound class distributions to different degrees. Some compound classes in O_2 -species are also called naphthenic acids, which are represented by the general formula described by $\text{C}_n\text{H}_{2n+z}\text{O}_2$. The Z value is equal to 0 for saturated linear hydrocarbon chains, and changes to -2 in monocyclic naphthenic acids, -4 in bicyclic, -6 in tricyclic, and so on. The O_4 compounds are suggestive of diacids.

3.6. Z-series distributions of O_2 compounds

The O_2 class is usually chosen to monitor crude oil biodegradation process because it is widely present in biodegraded oils and plays a critical role as an intermediate in many common crude oil conversion reactions [20]. The type analysis of O_2 -species, expressed as a Z distribution, is illustrated in Fig. 5. Great changes can be observed in Z -series abundance of O_2 compounds. The non-treated residues exhibited high relative abundance of naphthenic acids. The treated residues contained the highest relative abundance of acyclic acids at 11.02%, followed by monocyclic and bicyclic naphthenic acids at 4.21% and 2.77%, respectively. It is

quite interesting to note that acyclic acids became the predominant class after oxidation, compared to the general decrease in the relative abundance of other classes. Han et al. [25] observed a general structure–persistence relationship which indicated that increased cyclization (Z) reduced the biodegradation rate for naphthenic acids in mixtures. In the present study, however, acyclic acids seemed to be more recalcitrant to the Fenton-like reaction than other Z -series. Considering that Fenton' reagent is a very powerful and somehow indiscriminate oxidizing agent, the increased relative abundance of acyclic acids might be due to the transformation, such as ring cleavage, of other classes into $Z=0$ series. However, it would be quite difficult to determine the concrete process of structural conversion in such a highly complex mixture.

Naphthenic acids are weakly biodegradable and are toxic to aquatic algae and other microorganisms [8]. Moreover, Atlas and Bartha [6] found that biodegradation of petroleum might be inhibited in the presence of fatty acids. As described above, reduction of the contamination level in the soil had reached a plateau during the previous bioremediation process, which might be due to inhibited degradative activity of the microorganisms caused by the high level of naphthenic acids.

3.7. Carbon number distributions for acyclic naphthenic acids

Fig. 6 shows the carbon number distributions for acyclic naphthenic acids. The carbon number, indicating the degree of alkyl substitution, ranged from 13 to 52 but lacked 44 to 51 for the non-treated sample. After oxidation treatment, the carbon number ranged from 13 to 48 but lacked 45. As shown in Fig. 6, both samples exhibited a maximum abundance at C_{28} . In addition, all series except C_{16} showed increased relative abundance after Fenton-like treatment. As a result of oxidation, there had been a major increase in the proportion of acyclic naphthenic acids ($\text{C}_n\text{H}_{2n}\text{O}_2$) and a decrease in O_2 species (Table 3 and Fig. 6). This clearly shows preferential removal of unsaturated and cyclic species. Of course, removal efficiency varied with the carbon number within $\text{C}_n\text{H}_{2n}\text{O}_2$ compounds

3.8. The two-dimensional van Krevelen diagram for N_1 and N_2 species

The two-dimensional van Krevelen graph (Fig. 7) was constructed for those species that contained one and two nitrogen

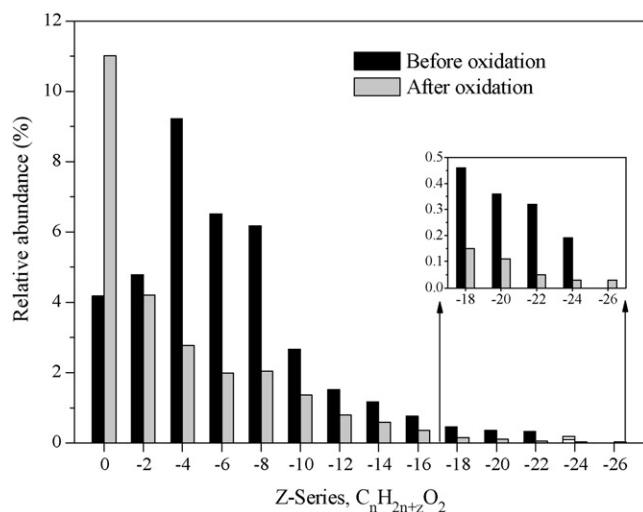


Fig. 5. Z -series abundance distribution of $\text{C}_n\text{H}_{2n+z}\text{O}_2$ compounds. ^{12}C and ^{13}C iso-mers are combined. Inset shows expanded vertical scale.

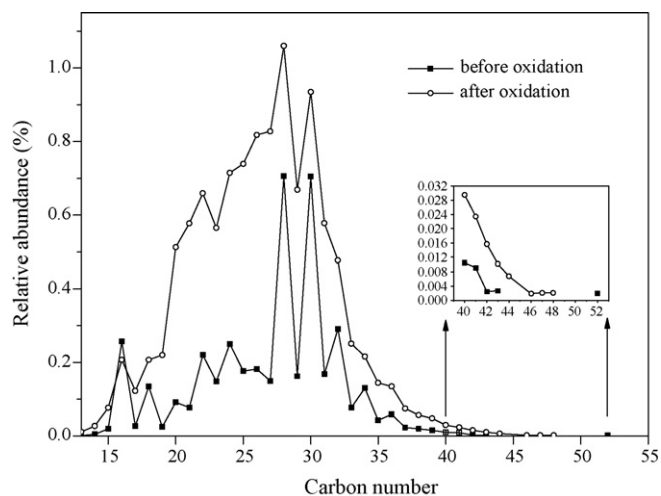


Fig. 6. Carbon number distributions for $C_nH_{2n}O_2$ compounds. ^{12}C and ^{13}C isomers are combined. The carbon number ranges from 13 to 52. Inset shows expanded vertical scale.

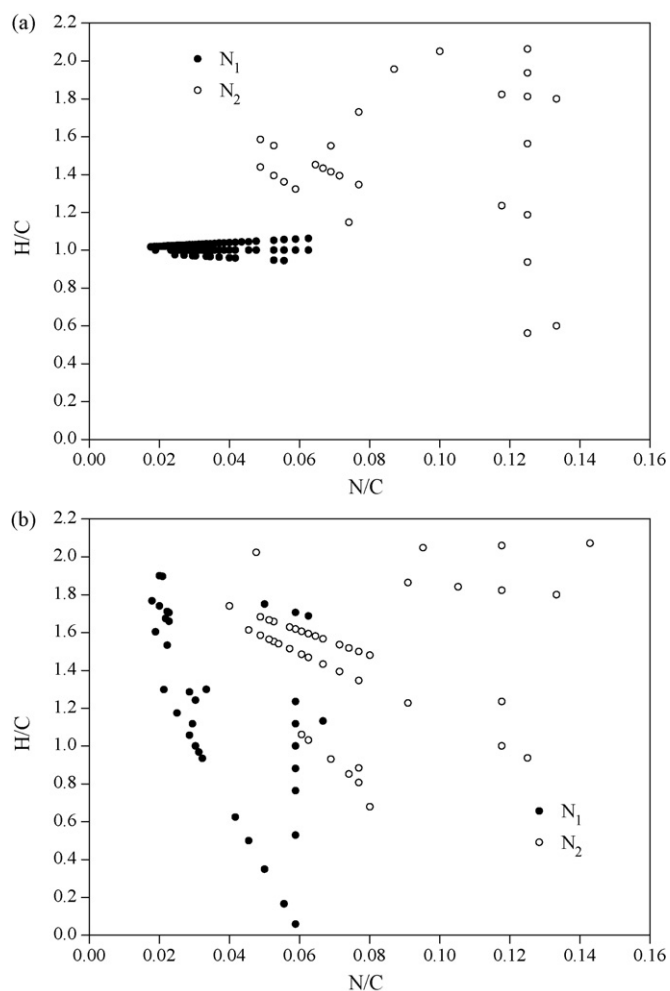


Fig. 7. The two-dimensional van Krevelen diagram for nitrogen only-containing classes identified in the residues. (a) Before oxidation, and (b) after oxidation.

atoms, by plotting the atomic ratios of N/C on the x -axis and H/C on the y -axis. It is clear that there were obvious blank spaces in the plot. One of the reasons for the pattern could be attributed to limitations in numbers of carbon, hydrogen, and nitrogen atoms in the

Table 2

Changes in the number of N_xO_y peaks identified before and after Fenton-like treatment.

Species	The number of peaks	
	Before oxidation	After oxidation
N_1O_1	117	184
N_1O_2	518	47
N_1O_3	107	92
N_1O_4	181	192
N_2O_2	346	248
N_2O_4	188	227
N_2O_5	337	396
N_5O_3	337	104
N_6O_2	695	622
N_7O_3	643	306
Sum	3469	2418

observed peaks. Moreover, the numbers of hydrogens were only odd numbers for N_2 -species. Because of these limitations, points could not exist in certain areas of the plot.

As shown in Fig. 7, there had been substantial changes in molecular compositions as the chemical treatment proceeded. There were 260 peaks in N_1 -species (Fig. 7a), however it dropped to 67 after Fenton-like oxidation, indicating that the N–H or C–N bonds were destroyed substantially by radicals. Moreover, the Z-number of N_1 -species ranged from -15 to -45 at intervals of 2 before treatment, which was altered to a series of smaller values (-5 , -13 , -15 , -17 , -19 , -21 , -25 , -30 , and -33). This decline in Z-number suggested that some condensed rings were cracked in free-radical reactions. For N_2 -species, there were 32 and 58 peaks before and after treatment, respectively. These increasing peaks in N_2 -species might be formed by chemical conversion of other nitrogen and oxygen-containing compounds such as N_2O_2 , N_2O_4 and N_5O_3 species, etc.

As can be seen in Fig. 7a, most of the peaks in N_1 -species were located in the narrow zone where H/C ratios were around 1, and N/C ratios were between 0.015 and 0.040. However, the peaks in N_1 -species were scattered over a broad zone along after oxidation treatment (Fig. 7b), and some peaks with H/C ratios over 1 appeared. As shown in Table 2, a significant reduction in the number of N_xO_y peaks was observed. We speculated that some other species had been transformed into N_1 -species. In this study, complete mineralization of a certain species would be difficult to obtain, considering that there were still 2300 mg TEO remaining in per kg soil at the end of treatment.

3.9. The two-dimensional van Krevelen diagram for N_1O_2 -species

Elemental compositions for N_1O_2 -species in bioremediation residues extract are represented in the van Krevelen diagram of Fig. 8. As shown earlier, there was a great change in the relative abundance of N_1O_2 -species during soil treatment (Table 3). Moreover, the number of peaks in N_1O_2 class, surprisingly, dropped from 518 to 47 after the Fenton-like treatment (Table 2). The disposition of N_1O_2 -species varied according to Z-series and degree of alkylation. N_1O_2 -species with Z values of -17 , -19 and -25 retained a few peaks, while other Z-series were eliminated completely in the Fenton-like reaction. Some new species with higher H/C ratios were also formed.

The biorefractory nature of many persistent organic pollutants has resulted in efforts to devise chemical and physical methods of degrading pollutants in contaminated sites such as soils, sediments, and groundwater [26]. Fenton reagent has been applied to the degradation of a wide variety of pollutants, predominantly persistent organic pollutants. In Fenton reactions, substituted aromatics can react either by addition of hydroxyl radical to the aromatic

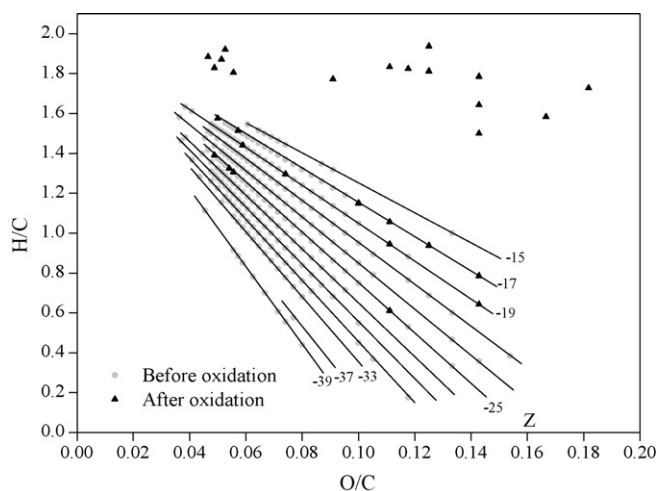


Fig. 8. The two-dimensional van Krevelen diagram for N_1O_2 -species identified in the residues.

Table 3

Relative abundances (%) of compound species identified in TEO. For simplicity, species are abbreviated to represent only the heteroatom content. ^{12}C and ^{13}C are combined.

Compound species	Before oxidation	After oxidation
O_1	0.99	2.37
O_2	38.34	25.49
O_3	2.03	14.34
O_4	0.66	0.59
O_5	1.75	3.40
O_8	0.14	0.38
N_1	1.78	5.65
N_2	0.06	0.23
N_1O_1	0.61	1.20
N_1O_2	5.59	0.13
N_1O_3	0.38	0.28
N_1O_4	0.65	0.70
N_2O_2	2.69	2.52
N_2O_4	2.57	1.52
N_2O_5	1.20	3.33
N_5O_3	1.62	0.28
N_6O_2	4.07	7.83
N_7O_3	7.54	9.98
Other	27.33	19.78

ring structure or by reaction with the ring substituents. Because the aromatic structure generally has a higher rate constant than alcohols, attack by hydroxyl radical to the ring is more prevalent [26]. In general, alkenes and aromatics react rapidly with hydroxyl radical, whereas alkanes react somewhat more slowly. As stated above, we observed great shifts in the distribution of N_1 and N_1O_2 species demonstrated by the 2D van Krevelen plot. Taking into consideration the above discussion, we could believe that a variety of species had undergone transformation of chemical structures in the Fenton-like reaction.

4. Conclusions

This study reported the capability of a Fenton-like reaction, using Fe^{3+} -EDTA as the catalyst, to destroy bioremediation residues in a highly petroleum-contaminated soil. This approach allowed the use of pH-neutral conditions thus avoiding acidification of the soil that could produce a strongly negative environmental impact. The Fenton-like treatment greatly reduced the contamination level in the soil. The pH of the reaction system was observed to have a major effect on the chemical oxidation efficiency of the residues in soil. Significant and detailed changes in the chemical composition

of polar compounds were revealed before and after treatment by the application of ESI FT-ICR MS. A fused ring compound identified as $C_{34}H_{38}N_1$ was found to make up a large part of the residues.

Acknowledgements

This work has been funded by the National Natural Science Foundation of China (40672211). The authors are grateful to Analysis Center, State Key Laboratory of Heavy Oil Processing, China University of Petroleum, for their technical assistance in FT-ICR MS analysis.

Appendix A. Supplementary data

Supplementary data associated with this article can be found, in the online version, at doi:10.1016/j.jhazmat.2010.03.046.

References

- [1] G. Płaza, G. Nałęcz-Jawecki, K. Ulfig, R.L. Brigmon, The application of bioassays as indicators of petroleum-contaminated soil remediation, *Chemosphere* 59 (2005) 289–296.
- [2] R.M. Atlas, *Petroleum biodegradation and oil spill bioremediation*, Mar. Pollut. Bull. 31 (1995) 178–182.
- [3] R. Boopathy, Factors limiting bioremediation technologies, *Bioresour. Technol.* 74 (2000) 63–67.
- [4] J.D. Van Hamme, A. Singh, O.P. Ward, Recent advances in petroleum microbiology, *Microbiol. Mol. Biol. Rev.* 67 (2003) 503–549.
- [5] R.C. Loehr, M.T. Webster, Performance of long-term, field-scale bioremediation processes, *J. Hazard. Mater.* 50 (1996) 105–128.
- [6] R.M. Atlas, R. Bartha, Inhibition by fatty acids of the biodegradation of petroleum, *Anton. Van Lee.* 39 (1973) 257–271.
- [7] D.T. Gibson, V. Subramanian, *Microbial Degradation of Organic Compounds*, Marcel Dekker Inc., New York, 1984.
- [8] D.W. McMartin, Persistence and fate of acidic hydrocarbons in aquatic environments: naphthenic acids and resin acids, Ph.D. Dissertation, University of Saskatchewan, Canada, 2003.
- [9] C.M. Miller, R.L. Valentine, M.E. Roehl, P.J.J. Alvarez, Chemical and microbiological assessment of pendimethalin-contaminated soil after treatment with Fenton's reagent, *Water Res.* 30 (1996) 2579–2586.
- [10] K. Nam, W. Rodriguez, J.J. Kukor, Enhanced biodegradation of polycyclic aromatic hydrocarbons by biodegradation combined with a modified Fenton reaction, *Chemosphere* 45 (2001) 11–20.
- [11] M.E. Lindsey, G. Xu, J. Lu, M.A. Tarr, Enhanced Fenton degradation of hydrophobic organics by simultaneous iron and pollutant complexation with cyclodextrins, *Sci. Total. Environ.* 307 (2003) 215–229.
- [12] A.C. Ndjou'ou, D. Cassidy, Surfactant production accompanying the modified Fenton oxidation of hydrocarbons in soil, *Chemosphere* 65 (2006) 1610–1615.
- [13] S.H. Kong, R.J. Watts, J.H. Choi, Treatment of petroleum-contaminated soils using iron mineral catalyzed hydrogen peroxide, *Chemosphere* 37 (1998) 1473–1482.
- [14] R.J. Watts, D.R. Haller, A.P. Jones, A.L. Teel, A foundation for the risk-based treatment of gasoline-contaminated soils using modified Fenton's reactions, *J. Hazard. Mater.* 76 (2000) 73–89.
- [15] L. Mater, E.V.C. Rosa, J. Berto, A.X.R. Corrêa, P.R. Schwingel, C.M. Radetski, A simple methodology to evaluate influence of H_2O_2 and Fe^{2+} concentrations on the mineralization and biodegradability of organic compounds in water and soil contaminated with crude petroleum, *J. Hazard. Mater.* 149 (2007) 379–386.
- [16] T.T. Tsai, C.M. Kao, Treatment of petroleum-hydrocarbon contaminated soils using hydrogen peroxide oxidation catalyzed by waste basic oxygen furnace slag, *J. Hazard. Mater.* 170 (2009) 466–472.
- [17] M. Lu, Z. Zhang, W. Yu, Z. Wei, Biological treatment of oilfield-produced water: a field pilot study, *Int. Biodeter. Biodegr.* 63 (2009) 316–321.
- [18] X. Xue, K. Hanna, C. Despas, F. Wu, N. Deng, Effect of chelating agent on the oxidation rate of PCP in the magnetite/ H_2O_2 system at neutral pH, *J. Mol. Catal. A: Chem.* 311 (2009) 29–35.
- [19] P.M. Rutherford, D.K. Banerjee, S.M. Luther, M.R. Gray, M.J. Dudas, W.B. McGill, M.A. Pickard, M.J. Salloum, Slurry-phase bioremediation of creosote and petroleum-contaminated soils, *Environ. Technol.* 19 (1998) 683–696.
- [20] C.A. Hughey, S.A. Galasso, J.E. Zumberge, Detailed compositional comparison of acidic NSO compounds in biodegraded reservoir and surface crude oils by negative ion electrospray Fourier transform ion cyclotron resonance mass spectrometry, *Fuel* 86 (2007) 758–768.
- [21] M.B. Cassidy, K.T. Leung, H. Lee, J.T. Trevors, A comparison of enumeration methods for culturable *Pseudomonas fluorescens* cells marked with green fluorescent protein, *J. Microbiol. Meth.* 40 (2000) 135–145.
- [22] J.C. Lou, Y.J. Huang, Assessing the performance of wastewater treatment with the combination of Fenton and ferrite process, *Environ. Monit. Assess.* 151 (2009) 251–258.

- [23] J.P. Waddell, G.C. Mayer, Effects of Fenton's reagent and potassium permanganate application on indigenous subsurface microbiota: a literature review, Proceedings of the 2003 Georgia Water Resources Conference, held April 23–24, 2003, at the University of Georgia.
- [24] D. Lin-Vien, N.B. Colthup, W.G. Fateley, J.G. Grasselli, The Handbook of Infrared and Raman Characteristic Frequencies of Organic Molecules, Academic Press, New York, 1991.
- [25] X. Han, A.C. Scott, P.M. Fedorak, M. Bataineh, J.W. Martin, Influence of molecular structure on the biodegradability of naphthenic acids, Environ. Sci. Technol. 42 (2008) 1290–1295.
- [26] M.A. Tarr, Chemical Degradation Methods for Wastes and Pollutants: Environmental and Industrial Applications, Marcel Dekker Inc., New York, 2003.